Bioorganic Chemistry 84 (2019) 363–371

Contents lists available at ScienceDirect

Bioorganic Chemistry

journal homepage: www.elsevier.com/locate/bioorg

Multi-target inhibitors against Alzheimer disease derived from 3-hydrazinyl 1,2,4-triazine scaffold containing pendant phenoxy methyl-1,2,3-triazole: Design, synthesis and biological evaluation

Mahnaz Yazdani[a,b], Najmeh Edraki[c,*], Rashid Badri[b], Mehdi Khoshneviszadeh[c], Aida Iraji[c], Omidreza Firuzi[c]

[a] Department of Chemistry, Khozestan Science and Research Branch, Islamic Azad University, Ahvaz, Iran
[b] Department of Chemistry, Ahvaz Branch, Islamic Azad University, Ahvaz, Iran
[c] Medicinal and Natural Products Chemistry Research Center, Shiraz University of Medical Sciences, Shiraz, Iran

ARTICLE INFO

Keywords:
Alzheimer's disease
BACE1
Antioxidant
Metal chelator
1,2,4- triazine
Phenoxy methyl-1,2,3- triazole
Neuroprotection

ABSTRACT

Alzheimer's disease (AD) is a complex neurological disorder with diverse underlying pathological processes. Several lines of evidence suggest that BACE1 is a key enzyme in the pathogenesis of AD and its inhibition is of particular importance in AD treatment. Ten new 3-hydrazinyl-1,2,4-triazines bearing pendant aryl phenoxy methyl-1,2,3-triazole were synthesized as multifunctional ligands against AD. We show that compounds containing Cl and NO_2 groups at the para position of the phenyl ring, namely compounds **7c** (IC_{50} = 8.55 ± 3.37 μM) and **7d** (IC_{50} = 11.42 ± 2.01 μM), possess promising BACE1 inhibitory potential. Furthermore, we assessed the neuroprotective activities of **7c** and **7d** derivatives in PC12 neuronal cell line, which showed moderate protection against amyloid β peptide toxicity. In addition, compound **7d** demonstrated metal chelating activity and moderate antioxidant potential (IC_{50} = 44.42 ± 7.33 μM). Molecular docking studies of these molecules revealed high-affinity binding to several amino acids of BACE1, which are essential for efficient inhibition. These results demonstrate that 1,2,4-triazine derivatives bearing an aryl phenoxy methyl-1,2,3-triazole have promising properties as therapeutic agents for AD.

1. Introduction

Alzheimer's disease (AD) is the most prevalent neurodegenerative disorder. It is the sixth leading cause of death in the United States and poses a significant economic burden [1]. The pathology of AD is not fully understood, but diverse factors including the formation of amyloid plaques, neurofibrillary tangles consisting of hyperphosphorylated tau protein, neuroinflammation, oxidative stress and dyshomeostasis of biometals are associated with AD [2–4]. Currently, there is no definitive disease-modifying treatment available for AD and therapeutic approaches only slow down neurodegeneration [5,6]. Therefore, there is an urgent need to discover novel therapeutic methods that target the core pathology of the disease.

Recent evidence suggests that inhibition of BACE1, a type I transmembrane aspartic protease may be a promising approach to treat AD [7]. So far, many studies have examined peptide inhibitors of this enzyme [8,9]. However, peptide drugs or closely related analogs may face several impediments such as the inability to penetrate the blood-brain barrier, low bioavailability and susceptibility to efflux by p-glycoprotein [7]. To overcome these problems, inhibitors with a small and non-peptide chemical structure have been designed and synthesized without the limitations of peptide inhibitors [10].

In addition to BACE1 inhibition, chelation therapy as a novel method of therapeutic intervention has been investigated in many CNS disorders including AD, Parkinson disease and multiple sclerosis [11]. This may be in part explained by the association between increased deposits of biometal cations to changes that lead to degeneration. The protective effects of metal chelators are based on trapping Fe, Cu, Zn ions [12–14].

Furthermore, oxidative stress has been also considered as a crucial contributing factor in the pathogenesis of AD [15,16]. Generation of reactive oxygen species (ROS) and reactive nitrogen species (RNS) exacerbate neuronal and brain damage [17]. In this context, antioxidants would be of therapeutic value to AD.

In light of the notions mentioned above and to continue our efforts to achieve novel anti-Alzheimer agents [18–20], we have focused on

* Corresponding author.
E-mail address: edrakin@sums.ac.ir (N. Edraki).

https://doi.org/10.1016/j.bioorg.2018.11.038
Received 3 October 2018; Received in revised form 22 November 2018; Accepted 23 November 2018
Available online 29 November 2018
0045-2068/

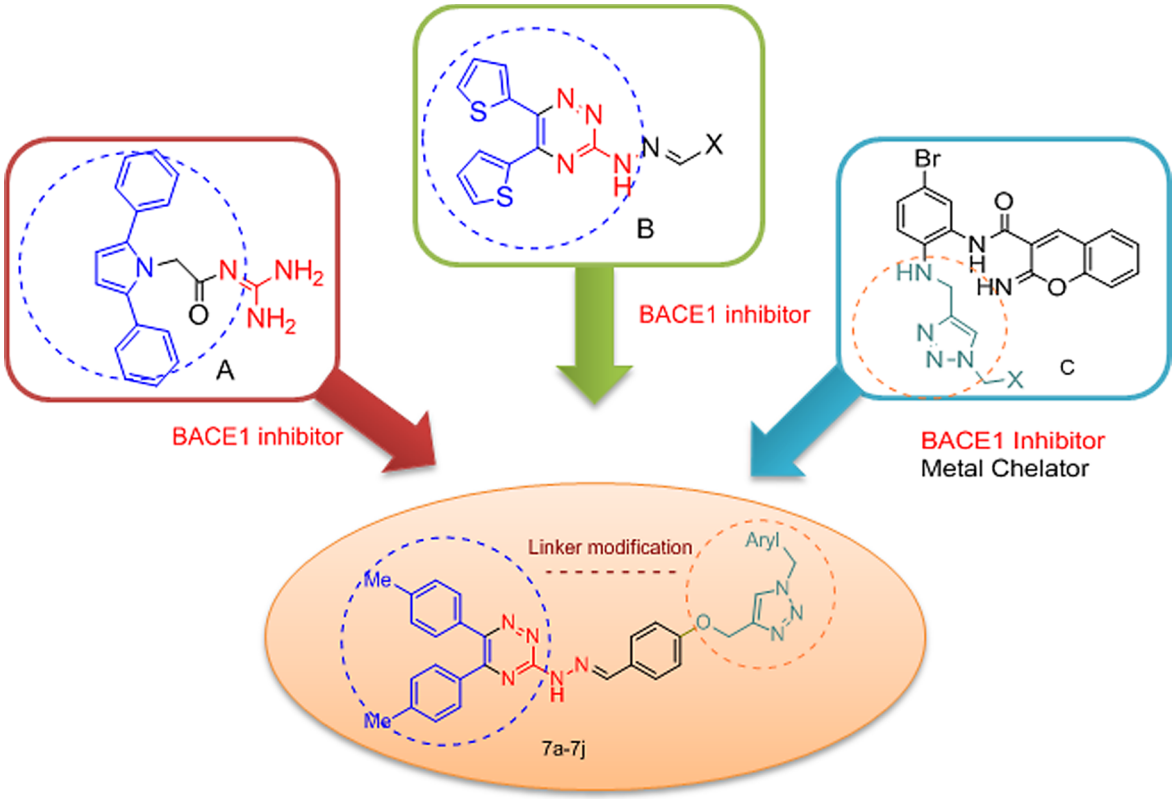

Fig. 1. Design strategy of target compounds as BACE1 inhibitor and metal chelating agent.

the synthesis, biological evaluation and computational analysis of a novel class of 3-hydrazynyl 1,2,4-triazine. We evaluated the synthesized compounds for their BACE1 inhibition, metal chelation, antioxidant and neuroprotective potential.

2. Results and discussion

2.1. Analogue-based pharmacophore design

Acylguanidine has been developed as a BACE1 inhibitor with IC_{50} of 3.7 μM. The X-ray structure of compound **A**, Fig. 1 with BACE1 demonstrated the key H bond interactions with the catalytic dyad. It seems that polar groups required for the enzyme's active site inhibition and improve BACE1 inhibition [21]. Recently, we characterized a series of 2-thiophene-2-yl-1,2,4-triazine **B**, Fig. 2 scaffolds as potent BACE1 inhibitors, with antioxidant and metal chelating potential. Structure-activity relationship (SAR) of this scaffold demonstrates that heteroaromatic moieties bearing H-bond donating atoms would enhance the BACE1 inhibitory potential (IC_{50} of 0.69 μM for the best compound) and improve antioxidant capacity (IC_{50} of 38.09 μM for the mentioned compound) [22]. The metal chelatory activity of Fe^{2+}, Fe^{3+}, Zn^{2+}, Cu^{2+} may be achieved by introducing triazole in the structure. Consequently, We used compound **B** as the starting point for further modification and optimization to target metal-Aβ species in AD [23]. We have also previously reported novel series of amino methylene triazole **C**, Fig. 3 with BACE1 inhibition, metal chelation and neuroprotective potential [24].

Hence, in the present work, we used a molecular hybridization

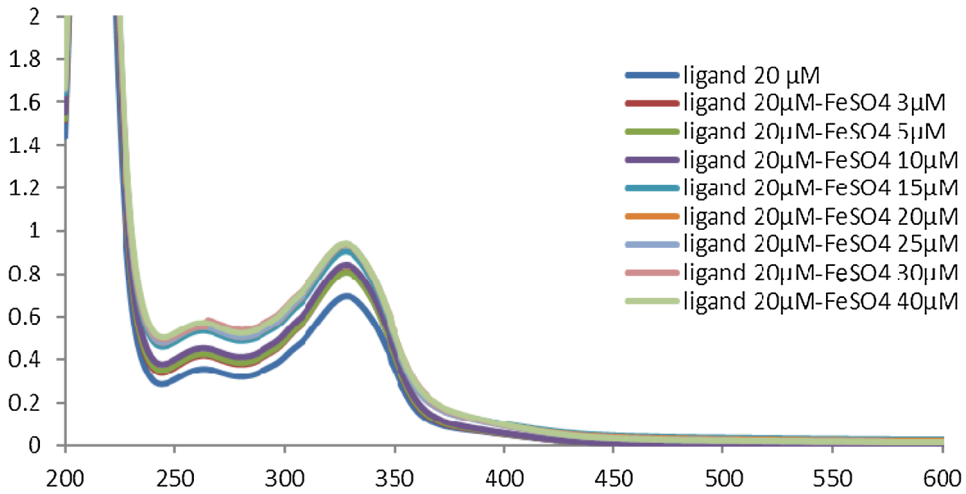

Fig. 2. The UV spectrum of compound **7d** alone or in the presence of, $FeSO_4$.

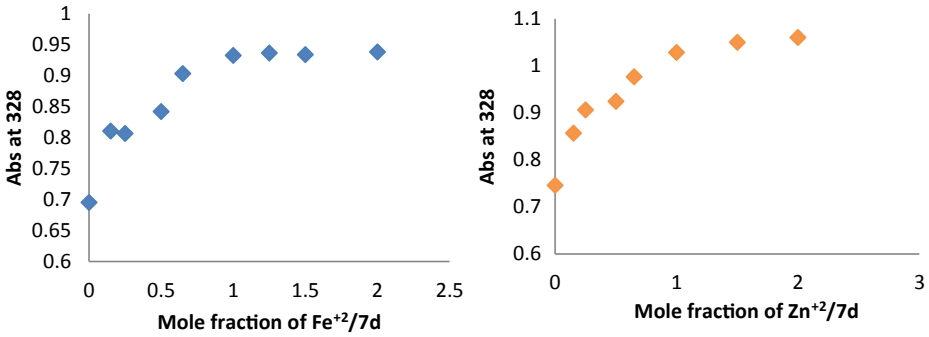

Fig. 3. Determination of the stoichiometry of complex-Fe^{+2} and Zn^{+2} using molar ratio method through titrating the methanol solution of compound **7d** with ascending amounts of $FeSO_4$ and $ZnSO_4$.

approach to design novel dual acting agents with BACE1 inhibition, neuroprotective and metal chelating properties. We assumed that replacing the thiophen groups (compound **B**) with phenyl ones would improve the compounds' accessibility to the BACE1 active site, while maintaining the hydrazine triazine linker for key H-bound interactions with the catalytic residue of the active site. The other structural modification involved the replacement of the amino methylene triazole (compound **C**) with oxo methylene triazole. Specifically, to increase favorable interactions, the nitrogen atom of the amino methylene linker was replaced with an oxygen atom. Moreover, to improve the metal chelating ability of the resulting compounds, we functionalized the triazole-ring at the C-4 position of the phenyl group. Different aryl substitutes were introduced at the triazole motif to better construct the Structure-activity relationship (SAR) of the designed scaffold.

2.2. Chemistry

The synthetic route to target compounds **7a–7j** is represented in Scheme 1. Reaction of benzil and hydrazinecarbothioamide in refluxing acetic acid resulted in compound **1** [25]. In the next step, the reaction of compound **1** and iodomethane in the presence of NaOH in EtOH at 25 °C resulted in the desired 3-(methylthio)-5,6-diphenyl-1,2,4-triazine **2** [22]. Reaction of compound **2** with hydrazine hydrate refluxing EtOH gave 3-hydrazineyl-5, 6-diphenyl-1,2,4-triazine **3** [16]. 4-(prop-2-yn-1-yloxy)benzaldehyde **4** was afforded via the reaction of 4-hydroxyaldehyde and 3-bromoprop-1-yne in the presence of K_2CO_3 in DMF at 80 °C. Further reaction of compound **4** and **3** in EtOH gave (E)-5,6-diphenyl-3-(2-(4-(prop-2-yn-1-yloxy)benzylidene)hydrazineyl)-1,2,4-triazine **5**. Different substituted (bromomethyl)benzene derivatives were reacted with sodium azide in the presence of triethylamine in THF and H_2O at 70 °C. After around 30 min, intermediate compound **6a–j** was added to the mixture of reaction in the presence of catalytic amount of $CuSO_4{\cdot}5H_2O$ (10 mol%) and sodium (2R)-2-[(1S)-12-dihydroxyethyl]-4-hydroxy-5-oxo-2*H*-furan-3-olate (25 mol%). The resulting mixture was stirred at 50 °C and completion of the reaction was monitored by using TLC to give compounds **7a–7j**. The chemical structure and some physical properties of synthesized derivatives are presented in Table 1.

2.3. In vitro inhibition of BACE1 enzyme

All synthesized compounds **7a–7j** were screened for their BACE1 inhibitory activity using an *in vitro* FRET-based technique. In an attempt to find potent BACE1 inhibitors, we synthesized a focused library of (E)-

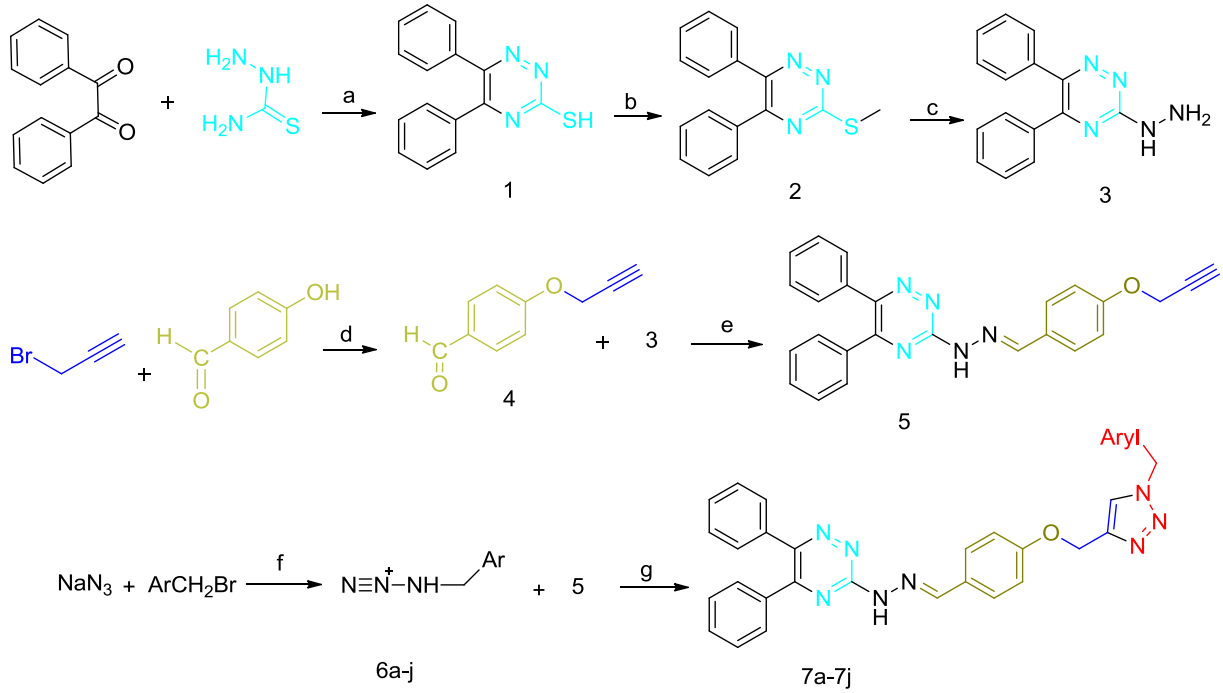

Scheme 1. Reagent: (a) CH_3COOH, EtOH, 2 h, Reflux. (b) NaOH, CH_3I, EtOH, 4 h, 25 °C. (c) $NH_2NH_2{\cdot}H_2O$, EtOH, 12 h, Reflux. (d) K_2CO_3, DMF, 80 °C, 18 h. (e) EtOH, 70 °C. (f) TEA, THF/water, 70 °C. (g) $CuSO_4{\cdot}5H_2O$ (10 mol%) and sodium (2R)-2-[(1S)-12-dihydroxyethyl]-4-hydroxy-5-oxo-2*H*-furan-3-olate (25 mol%), at 50 °C.

Table 1
Chemical structures and physical properties of the synthesized compounds 7a–7j.

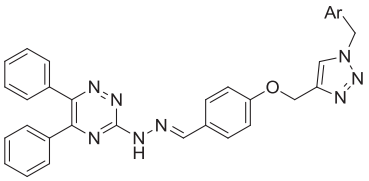

Compound	Ar	M.p. (°C)	Yield (%)
7a	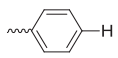	235–241	91
7b	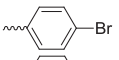	248–251	96
7c	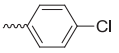	228–233	93
7d	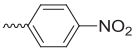	228–231	84
7e	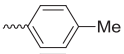	227–229	76
7f	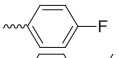	232–237	88
7 g	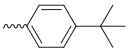	240–237	95
7 h	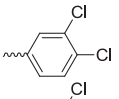	230–234	94
7i		241–245	87
7j	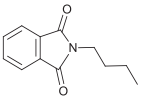	240–243	85

3-(2-(4-((1*H*-1,2,3-triazol-4-yl)methoxy)benzylidene)hydrazinyl)-5,6-diphenyl-1,2,4-triazine derivatives. The BACE1 inhibitory activities of these compounds are displayed in Table 2. OM99-2 (Glu-Val-Asn-Leu-Ala-Ala-Glu-Phe) was used as a reference BACE1 inhibitor.

Notably, the unsubstituted phenyl derivative **7a** had considerable inhibitory effect against BACE1 (IC_{50} = 18.77 μM, 58.32% inhibition at 30 μM).

To investigate the effect of substituted moiety on phenyl ring, different groups were introduced at para position of pendant phenyl. It was found that introduction of bulky electron withdrawing substituted group such as Cl (**7c**) and Br (**7b**) resulted in increased inhibitory potential of compounds; particularly **7c** showed an IC_{50} value of 8.55 μM with 79.17% inhibition at 30 μM. on the other hand **7f** bearing pendant fluorobenzyl demonstrate less inhibitory potential (16.81% inhibition at 30 μM) compared to **7c** and **7b**.

The promising activity of **7c** as the most potent compound led us to shift our focus toward finding the suitable position for the Cl group on the phenyl ring. Cl was substituted at various position of the pendant phenyl. 3-clorophenyl (**7i**) (37.04% inhibition at 30 μM) and 3,4 dicholoro phenyl (**7 h**) (42.16% inhibition at 30 μM) exhibited lower inhibitory activity in comparison with **7c**.

Subsequently, the inhibitory effect of electron donating groups was further evaluated. Introduction of a methyl group (**7e**) diminished the activity (30.04% inhibition at 30 μM) compared to an unsubstantiated one (**7a**). In order to confirm the necessity of optimum bulkiness, the methyl group was replaced with *t*-butyl at 4 position. These results clearly depicted that *t*-butyl contributed to a higher BACE1 inhibitory activity with IC_{50} = 24.58 μM (63.59% inhibition at 30 μM)

With the promising results on the BACE1 inhibitory activity of our nitro substituted derivatives as hydrogen bond interacting motif [22], the potency of nitro phenyl derivatives was investigated . The outcome implies the superior inhibitory activity of the nitro group at para position of pendant phenyl (**7d**) (IC_{50} = 11.42 μM, 77.08% inhibition at 30 μM).

Based on enzymatic inhibitory activity, **7j** containing propylisoindoline fragment with IC_{50} = 18.08 μM (67.09% inhibition at 30 μM) emerged as the other interesting inhibitor of the series, producing a substantial improvement of BACE1 inhibition potency.

2.4. DPPH radical scavenging activity

The *in vitro* antioxidant activity of the synthesized compounds was tested by the 1,1-diphenyl-2-picrylhydrazyl (DPPH) radical scavenging assay as a widely accepted method to evaluate the antioxidant effect. A screen was performed at the concentrations of 30, 100 and 300 μM and quercetin was used as the reference compound. Amongst the compounds screened for DPPH radical scavenging activity, **7d** containing a nitro motif showed a modest antioxidant effect with an IC_{50} value of 44.42 μM.

2.5. Neuroprotective activity against $A\beta_{25\text{-}35}$-induced cell death in PC12 neurons

The cleavage of amyloid precursor protein (APP) generates amyloid β-peptide (Aβ), which can be toxic to neuronal cells. Aβ may also induce the production of reactive oxygen species (ROS) and has a central role in the pathogenesis of AD [26]. To test the neuronal protective activity of our two selected compounds against $A\beta_{25\text{-}35}$-induced damage, we used the MTT assay to examine toxicity in PC12 neuronal cell line. Our results show that compounds **7c** and **7d** have moderate neuroprotective activity at 5 μM (10% protection for **7c** and 14% protection for **7d**).

2.6. Metal chelation

The ability of the synthesized compounds in chelating metals would be an added advantage in the treatment of AD. To test the metal-chelating effect of our compounds, we used compound **7d** as an example to chelate biometals such as Zn^{2+} and Fe^{2+} in wavelengths ranging from 200 to 700 nm. As shown in Fig. 2, after the addition of either $FeSO_4$ or $ZnSO_4$ to a solution of **7d**, there was no obvious optical shift; however, the dramatic increase in absorbance indicated a possible interaction between these biometals and the ligand. This suggests that compound **7d** is able to chelate biometals.

To determine the stoichiometry of compound **7d** in complex with the biometals mentioned above, we used the mole ratio method by preparing solutions of compound **7d** (20 μM) and metal ions ranging from 0 to 60 μM. The UV spectra were recorded and the absorbance change at 328 nm was plotted against the mole fraction of compound **7d**, resulting in two straight lines. As shown in Fig. 3, the absorbance linearly increased initially and then plateaued. The two straight lines intersected at a mole fraction of 1, indicating a 1:1 stoichiometry for the **7d**-Fe^{+2} and **7d**-Zn^{+2} complexes.

2.7. Docking study

We next sought to confirm the *in vitro* enzymatic inhibition results of our synthesized compounds against BACE1 by performing molecular docking studies. First, the ligand of Co-crystallized 1W51 was re-docked to the binding site of the protein structure to validate the docking protocol. The RMSD value of re-docking in the binding cavity of the enzyme was 1.46. Based on the standard and accepted RMSD value (less than 2.00 Å), it was concluded that the docking protocol is acceptable for the analysis of binding modalities of the investigated compounds. (See the supplementary data Table 3 for all docked results). In almost all active structure, hydrazine linker depicted hydrogen bonds

Table 2
Results of BACE1 inhibitory and antioxidant effects of the synthesized compounds.

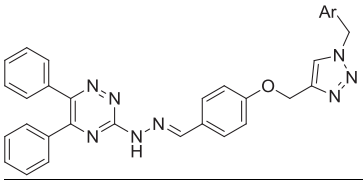

Compound	Ar	IC_{50} μM (± SE)[a]	% Inhibition at 30 μM (± SE)[a]	% Inhibition at 10 μM (± SE)[a]	IC_{50} μM (± SE)[a]
		BACE1 Assay			DPPH assay
7a	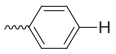	18.77 ± 2.68	58.32 ± 6.40	29.98 ± 5.62	> 50
7b	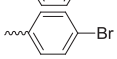	24.09 ± 3.36	54.09 ± 4.40	33.37 ± 7.98	> 50
7c	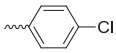	8.55 ± 3.37	79.17 ± 5.01	58.94 ± 11.56	> 50
7d	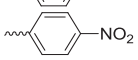	11.42 ± 2.01	77.08 ± 8.88	45.54 ± 6.43	44.42 ± 7.33
7e	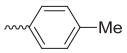	–	30.04 ± 7.37	15.23 ± 3.12	> 50
7f	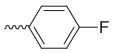	–	16.81 ± 5.55	11.44 ± 13.67	> 50
7g	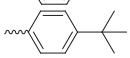	24.58 ± 5.90	63.59 ± 10.14	29.98 ± 7.69	> 50
7h	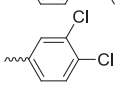	–	42.16 ± 2.72	37.72 ± 1.50	> 50
7i		–	37.04 ± 3.14	28.49 ± 4.75	> 50
7j	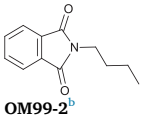	18.05 ± 4.30	67.09 ± 8.74	35.51 ± 4.76	> 50
	OM99-2[b]	14.7 (± 2.8) (nM)			
	Quercetin[c]				4.62 (± 2.26)

[a] Data presented here are the mean ± S.E.M. of three to six independent experiments
[b] OM99-2 was used as positive control.
[c] Quercetin was used as a standard positive control.

interactions with Asp32 and 228 crucial for the efficient inhibition of BACE1. The bi-phenyl forms hydrophobic interaction with residues in S'2 pocket and different pendant (hetero) aryl oriented toward S2 pocket

Our docking study showed that compound **7d** had the lowest binding energy of -13.63 kcal mol^{-1}. The lowest energy pose of **7d** demonstrated hydrogen bond interaction with the side chain residues Asp32, Asp228, Asn233 and Arg235 within the active site (Fig. 4). Strong hydrogen bond interactions were found with two key catalytic residues: (I) the NH group of hydrazine linker and the oxygen atom of Asp228 (II) N atom of hydrazine linker accepted hydrogen from OH group of Asp32. Three hydrogen bond interactions were observed between Asn233 and Arg235 with the nitro group attached at the para position of the pendant phenyl. Moreover, the triazine ring showed Π-Π stacking interaction with Tyr71of the S1 sub-pocket. In fact, the interaction with Tyr71 is the key element for the open and closed conformations of BACE1 [27]. Binding modes of another promising compound, **7c** (Fig. 5), showed that **7c** was also involved in H-bond interaction between hydrazine linker and Asp228 and Asp32. Furthermore, the triazine ring was accommodated in the S1 pocket and Π-Π stacking interaction was observed with Tyr71.

3. Conclusion

Here, we report the design and synthesis of a new series of 3-hydrazynyl 1,2 4-triazine derivatives as multitarget structures for managing AD. Some of our synthesized compounds were strong inhibitors of BACE1. The key structural feature that enabled BACE1 inhibition was the presence of electron withdrawing groups at the para position of the phenyl ring. More specifically, derivatives containing Cl and NO_2 in the para position of the phenyl ring (**7c, 7d**, respectively) showed higher inhibitory activity compared to the unsubstituted analog **7a**. On the contrary, the replacement of the Cl by F and CH_3 groups reduced the inhibitory activity. Molecular docking analysis of compounds **7c** and **7d** showed that the high BACE1 inhibitory potential may be in part due to the hydrogen bond interactions with Asp32, Asp228 within catalytic cavity of the BACE1 active site. The triazine ring was accommodated in the S1 pocket and stabled via pi-pi stacking interactions with Tyr71. The bi-phenyl moiety occupied the S'2 pocket and different pendant (hetero) aryl group oriented toward the S2 pocket. Furthermore, our *in vitro* neuroprotective assay revealed that compounds **7c** and **7d** can protect cells from toxic $A\beta_{25-35}$ species to various degrees. Additionally, the metal chelatory properties of the most potent compound (**7d**) was confirmed using the mole ratio method. Antioxidant potential of all compounds was tested by the DPPH assay and the results showed that only compound **7d** can be regarded as antioxidant with an IC_{50} value of 44.42 μM. In addition, the summarized SAR provided insights for the further development of specific BACE1 inhibitors. More specifically, **7c** and **7d** can be relevant starting compounds to achieve therapeutic agents against AD.

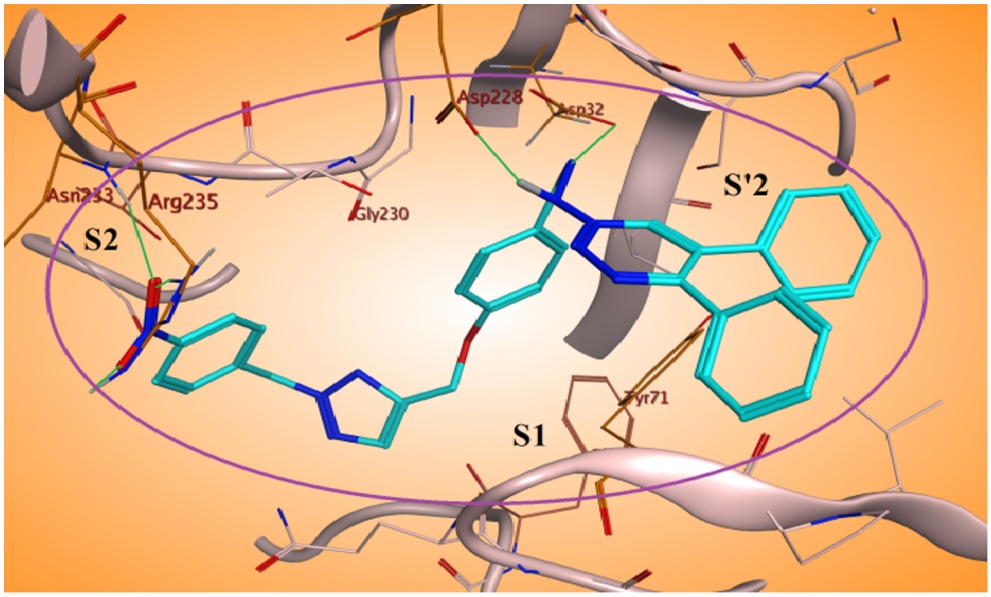

Fig. 4. 3D docking pose showing interaction for compound **7d** (blue) in the binding site of BACE1.

4. Materials and methods

4.1. Chemistry

All reagents were purchased from the suppliers (Sigma-Aldrich, Fluka and Merck) without further purification. Reaction progress was observed by thin layer chromatographyon on the glass-backed silica gel sheets (Silica Gel 60 GF254) and visualized under UV light (254 nm). Melting points were taken on Thermo Scientific Electrothermal digital apparatus (Thermo Fisher Scientific Inc.). ^{1}H NMR (300 or 500 MHz) and ^{13}C NMR (100 or 125 MHz) spectra were recorded on a Bruker AV-300 or 500 (300 or 500 MHz) spectrometer at ambient temperature. FT-NMR spectrometer are expressed in (δ, ppm) from the solvent resonance ($CDCl_3$, DMSO-d_6 2.50 ppm). Mass spectra were obtained on SHIMA-DZU LC-MS 2010 spectrometer. The infrared (IR) spectra were run as KBr disk on Perki- Elmer Spectrum RXI FTIR spectrophotometer.

4.1.1. Synthesis of 5,6-diphenyl-1,2,4-triazine-3-thiol (1)

Benzyl (37 mmol) was added to 60 ml of acetic acid and the mixture was heated to about 100 °C with stirring. Hydrazinecarbothioamide (75.04 mmol) was added and the mixture was refluxed for about 2 h. After cooling, the solid was filtered and washed with cold acetic acid and water. Orange solid; Yield: 88%; mp: 234–236 °C, ^{1}H NMR (300 MHz, DMSO-d_6) δ_H (ppm): 7.34 (m, 10H, Ar—H), 15.18 (s, 1H, S—H).

4.1.2. Synthesis of 3-(methylthio)-5, 6-diphenyl-1,2,4-triazine (2)

Sodium hydroxid (20 mmol) was dissolved in 60 ml of ethanol at 100 °C. The basic solution was cooled to room temperature and 5, 6-diphenyl-1,2,4-triazine-3-thiol (20 mmol) was added and stirred for 15 min. Afterward, iodomethane (47 mmol) was added drop wise to the reaction and stirred at room temperature for 4 h. After cooling, the precipitated solid was separated and recrystallized from ethanol to give

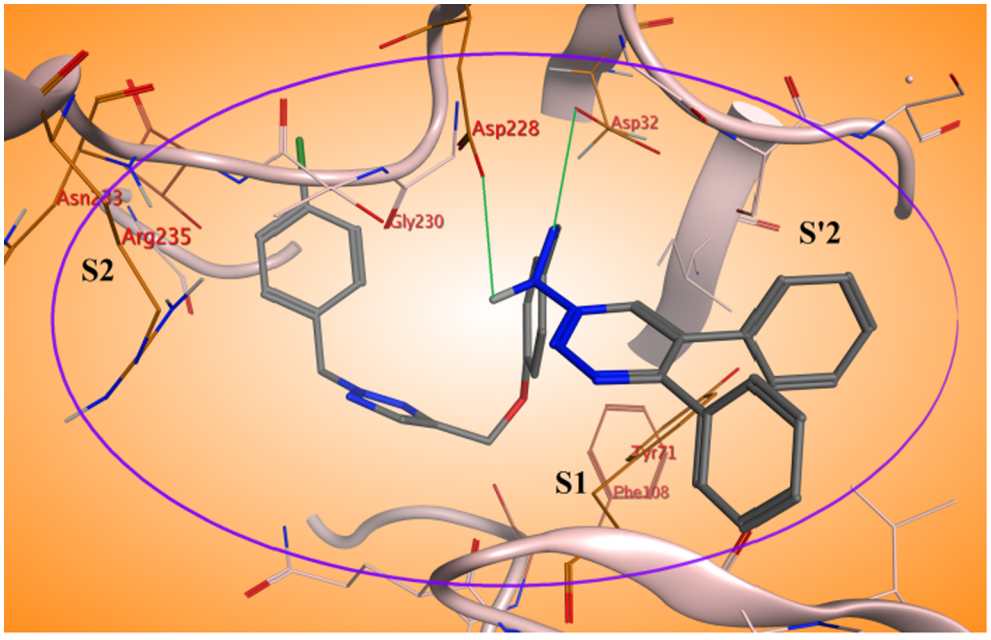

Fig. 5. 3D docking pose showing interaction for compound **7c** (grey) in the binding site of BACE1.

pure compound 3. Yellow solid; Yield: 90%, mp: 154–157 °C, ^{1}H NMR (300 MHz, DMSO-d_6) δ_H (ppm): 2.71 (s, 3H, S−C<u>H</u>$_3$), 7.40–7.92 (m, 10H, Ar−<u>H</u>).

4.1.3. Synthesis of 3-hydrazineyl-5, 6-diphenyl-1,2,4-triazine (3)

A mixture of 3-(methylthio)-5, 6-diphenyl-1,2,4-triazine (11.8 mmol) and NH_2 $NH_2{\cdot}H_2O$ (3 ml, 96 mmol) in 30 ml ethanol was refluxed for 12 h. After cooling, the precipitated solid was separated and washed with cold ethanol and recrystallized from ethanol to give 3-hydrazineyl-5,6-diphenyl-1,2,4-triazine. Dark yellow solid; Yield: 83%, mp: 182–185 °C, ^{1}H NMR (300 MHz, DMSO-d_6) δ_H (ppm): 4.49 (s, 1H, N−<u>H</u>), 6.70 (s, 2H, N<u>H</u>$_2$), 7.34 (m, 10H, Ar−<u>H</u>).

4.1.4. Synthesis of 4-(prop-2-yn-1-yloxy) benzaldehyde (4)

4-Hydroxybenzaldehyde (20 mmol), 3-bromoprop-1-yne (20 mmol) and K_2CO_3 (0.6 mmol) were dissolved in DMF (30 ml). The reaction mixture was mixed at 80 °C for 18 h. After cooling, the precipitate was filtered and washed with cold water and *n*-hexan, dried and give pure 4-(prop-2-yn-1-yloxy) benzaldehyde. Gray solid; Yield : 76%, mp:153–159 °C, ^{1}H NMR (300 MHz, DMSO-d_6) δ_H (ppm): 3.64 (s, 1H, ≡C−<u>H</u>), 4.89 (s, 2H, O−C<u>H</u>$_2$), 7.09 (d, 2H, J = 8.3 Hz, Ar−<u>H</u>), 7.82 (d, 2H, J = 8.3 Hz, Ar−<u>H</u>), 8.65 (s, 1H, CHO).

4.1.5. Synthesis of (E)-5,6-diphenyl-3-(2-(4-(prop-2-yn-1-yloxy) benzylidene)hydrazineyl)-1,2,4-triazine (5)

A mixture of 3-hydrazineyl-5,6-diphenyl-1,2,4-triazine (12 mmol) and 4-(prop-2-yn-1-yloxy) benzaldehyde (12 mmol) in ethanol (40 ml) was refluxed for 5 h. After cooling, the precipitated solid was separated and recrystallized from diethyl ether to give pure compound (E)-5,6-diphenyl-3-(2-(4-(prop-2-yn-1-yloxy)benzylidene)hydrazineyl)-1,2,4-triazine. Yellow solid: Yield 85%; mp: 211-214 °C, IR (KBr, cm^{-1}) ν: 1080, 1173, 1243, 1509, 1614, 2888, 3214, 3432. ^{1}H NMR (500 MHz, DMSO-d_6) δ_H (ppm): 3.63 (s, 1H, ≡C−<u>H</u>), 4.86 (s, 2H, C<u>H</u>$_2$), 7.06 (d, 2H, J = 8.8 Hz, Ar−<u>H</u>), 7.37–7.49 (m, 10H, Ar−<u>H</u>), 7.68 (d, 2H, J = 8.8 Hz, Ar−<u>H</u>), 8.24 (s, 1H, N=C−<u>H</u>), 11.87 (s, 1H, N−<u>H</u>),^{13}C NMR (125 MHz, DMSO-d_6) δ_c (ppm): 56.0, 78.9, 79.5, 115.7, 128.5, 128.7, 128.9, 129.4, 129.9, 130.7, 136.4, 136.6, 144.2, 151.1, 156.9, 158.7. MS m/z (%): 405 (M^+) (5), 248 (30), 178 (100).

4.1.6. Synthesis of substituted derivative of (E)-3-(2-(4-((1H-1,2,3-triazol-4-yl)methoxy)benzylidene)hydrazinyl)-5,6-diphenyl-1,2,4-triazine (6a–j)

Different derivatives of 5ai were prepared via the reaction of proper alkyl or aryl halide (1.1 mmol) with sodium azide (1 mmol) in the presence of triethylamine in THF/water. After around 30 min, (E)-5,6-diphenyl-3-(2-(4-(prop-2-yn-1-yloxy)benzylidene)hydrazineyl)-1,2,4-triazine (5) (1 mmol) in absolute THF (5 ml) was added to the solution in the presence of $CuSO_4{\cdot}5H_2O$ (10 mol%) and sodium (2R)-2-[(1S)-12-dihydroxyethyl]-4-hydroxy-5-oxo-2*H*-furan-3-olate (25 mol%), at 50 °C and stirred at 70 °C for 48 h. After completion of the reaction (checked by using TLC), the solvent was evaporated under vacuum and the residue was recrystallized from ethylacetate and *n*-hexan.

4.1.7. Synthesis of (E)-3-(2-(4-((1-benzyl-1H-1,2,3-triazol-4yl)methoxy) benzylidene) hydrazineyl)-5,6-diphenyl-1,2,4-triazine (7a)

White solid: Yield 91%; mp: 235–241 °C, IR (KBr, cm^{-1}) ν : 1081, 1168, 1239, 1500, 1610, 3032, 3435. ^{1}H NMR (500 MHz, DMSO-d_6) δ_H (ppm): 5.20 (s, 2H, N−C<u>H</u>$_2$−Ph), 5.62 (s, 2H, C<u>H</u>$_2$−O−Ph), 7.11 (d, 2H, J = 8.5 Hz, Ar−<u>H</u>), 7.32–7.49 (m, 15H, Ar−<u>H</u>), 7.67 (d, 2H, J = 8.5 Hz, Ar−<u>H</u>), 8.24 (s, 1H, N=C<u>H</u>), 8.32 (s, 1H, C=C<u>H</u>−N), 11.86 (s, 1H, N−<u>H</u>), ^{13}C NMR (125 MHz, DMSO-d_6) δ_c (ppm): 53.3, 61.6, 115.6, 125.3, 125.4, 128.1, 128.4, 128.6, 128.7, 129.2, 129.5, 129.9, 130.7, 136.5, 136.6, 139.7, 143.2, 144.0, 151.1, 156.8, 159.6. LC- MS (m/z):538 [M^+].

4.1.8. Synthesis of (E)-3-(2-(4-((1-(4-bromobenzyl)-1H-1,2,3-triazol-4-yl)methoxy)benzylidene)hydrazinyl)-5,6-diphenyl-1,2,4-triazine (7b)

Yellow solid: Yield %96; mp: 248–251 °C, IR (KBr, cm^{-1}) ν: 1068, 1081, 1167, 1237, 1508, 1610, 2923, 3228 . ^{1}H NMR (500 MHz, DMSO-d_6) δ_H (ppm): 5.20 (s, 2H, N−C<u>H</u>$_2$−Ph), 5.61 (s, 2H, C<u>H</u>$_2$−O−Ph), 7.11 (d, 2H, J = 8.3 HZ, Ar−<u>H</u>), 7.28 (d, 2H, J = 7.5 Hz, Ar−<u>H</u>), 7.37–7.49 (m, 10H, Ar−<u>H</u>), 7.58 (d, 2H, J = 7.5 Hz, Ar−<u>H</u>), 7.67 (d, 2H, J = 8.3 Hz, Ar−<u>H</u>), 8.24 (s, 1H, N=C−<u>H</u>), 8.32 (s, 1H, C=C<u>H</u>−N), 11.86 (s, 1H, N−<u>H</u>), ^{13}C NMR (125 MHz, DMSO-d_6) δ_c (ppm): 52.6, 84.5, 115.6, 121.9, 125.3, 126.8, 128.2, 128.6, 128.7, 128.8, 129.5, 129.9, 130.7, 131.3, 132.2, 135.7, 136.5, 136.6, 138.4, 143.3, 156.8. LC- MS (m/z):616 [M^+].

4.1.9. Synthesis of (E)-3-(2-(4-((1-(4-chlorobenzyl)-1H-1,2,3-triazol-4-yl)methoxy) benzylidene) hydrazineyl)-5,6-diphenyl-1,2,4-triazine (7c)

White solid: Yield %93, mp: 228–233 °C, IR (KBr, cm^{-1}) ν: 1057, 1082, 1168, 1240, 1507, 1610, 3000, 3429. ^{1}H NMR (500 MHz, DMSO-d_6) δ_H (ppm): 5.20 (s, 2H, N−C<u>H</u>$_2$−Ph), 5.63 (s, 2H, C<u>H</u>$_2$−O−Ph), 7.11 (d, 2H, J = 8.0 Hz, Ar−<u>H</u>), 7.35–7.48 (m, 14H, Ar−<u>H</u>), 7.67 (d, 2H, J = 8.0 Hz, Ar−<u>H</u>), 8.24 (s, 1H, N=C−<u>H</u>), 8.33 (s, 1H, C=C<u>H</u>−N), 11.86 (s, 1H, N−<u>H</u>), ^{13}C NMR (125 MHz, DMSO-d_6) δ_c (ppm): 52.5, 61.6, 115.6, 128.6, 128.7, 128.8, 129.0, 129.2, 129.4, 129.5, 129.9, 130.4, 133.4, 135.5, 136.5, 136.7, 143.3, 144.3, 146.6, 156.8, 159.6 . LC- MS (m/z): 573 [M^+].

4.1.10. Synthesis of (E)-3-(2-(4-((1-(4-nitrobenzyl)-1H-1,2,3-triazol-4-yl) methoxy) benzylidene) hydrazineyl)-5,6-diphenyl-1,2,4-triazine (7d)

Yellow solid: Yield %84; mp: 228–231 °C, IR (KBr, cm^{-1}) ν: 1080, 1170, 1239, 1347, 1508, 1610, 2924, 3430 .^{1}H NMR (500 MHz, DMSO-d_6) δ_H (ppm): 5.22 (s, 2H, N−C<u>H</u>$_2$−Ph), 5.82 (s, 2H, C<u>H</u>$_2$−O−Ph), 7.11 (d, 2H, J = 8.0 Hz, Ar−<u>H</u>), 7.37–7.55 (m, 14H, Ar−<u>H</u>), 7.67 (d, 2H, J = 8.0 Hz, Ar−<u>H</u>), 8.24 (s, 1H, C=C<u>H</u>−N), 8.39 (s, 1H, N=C−<u>H</u>), 11.86 (s, 1H, N−<u>H</u>), ^{13}C NMR (125 MHz, DMSO-d_6) δ_c(ppm): 52.4, 61.6, 115.6, 124.4, 125.7, 128.2, 128.6, 128.7, 128.8, 129.5, 129.5, 129.9, 130.7, 136.0, 136.6, 143.4, 143.8, 144.3, 147.7, 156.8, 159.5. LC- MS (m/z): 583 [M^+].

4.1.11. Synthesis of (E)-3-(2-(4-((1-(4-methylbenzyl)-1H-1,2,3-triazol-4-yl)methoxy) benzylidene) hydrazineyl)-5,6-diphenyl-1,2,4-triazine (7e)

Yellow solid, Yield; %76, mp: 227–229 °C, IR (KBr, cm^{-1}) ν: 1074, 1123, 1215, 1520, 1711, 2400, 2927, 3406. ^{1}H NMR (300 MHz, DMSO-d_6) δ_H (ppm): 1.35 (s, 3H, C<u>H</u>$_3$), 5.19 (s, 2H, N−C<u>H</u>$_2$−Ph), 5.62 (s, 2H, C<u>H</u>$_2$−O−Ph), 7.10 (d, 2H, J = 8.4 Hz, Ar−<u>H</u>), 7.20–7.47 (m, 14H, Ar−<u>H</u>), 7.66 (d, 2H, J = 8.4 Hz, Ar−<u>H</u>), 8.23 (s, 1H, C=C<u>H</u>−N), 8.31 (s, 1H, N=C−<u>H</u>), 11.85 (s, 1H, N−<u>H</u>), LC- MS (m/z): 552 [M^+].

4.1.12. Synthesis of (E)-3-(2-(4-((1-(4-fluorobenzyl)-1H-1,2,3-triazol-4-yl)methoxy) benzylidene) hydrazineyl)-5,6-diphenyl-1,2,4-triazine (7f)

Yellow solid: Yield %88; mp: 232–237 °C, IR (KBr, cm^{-1}) ν: 1123, 1168, 1240, 1509, 1608, 2869, 3214. ^{1}H NMR (500 MHz, DMSO-d_6) δ_H (ppm): 5.20 (s, 2H, N−C<u>H</u>$_2$−Ph), 5.61 (s, 2H, C<u>H</u>$_2$−O−Ph), 7.11 (d, 2H, J = 8.5 Hz, Ar−<u>H</u>), 7.20–7.49 (m, 14H, Ar−<u>H</u>), 7.67 (d, 2H, J = 8.5 Hz, Ar−<u>H</u>), 8.24 (s, 1H, N=C−<u>H</u>), 8.31 (s,1H, C=C<u>H</u>−N), 11.83 (s, 1H, N−<u>H</u>), ^{13}C NMR (125 MHz, DMSO-d_6) δ_c (ppm): 52.5, 61.6, 115.5, 125.2, 128.2, 128.6, 128.7, 129.5, 129.9, 130.8, 130.8, 132.7, 136.5, 136.7, 143.3, 144.3, 151.1, 156.8, 159.6, 161.4, 163.3. LC- MS (m/z): 556 [M^+].

4.1.13. Synthesis of (E)-3-(2-(4-((1-(4-(tert-butyl)benzyl)-1H-1,2,3-triazol-4-yl)methoxy) benzylidene)hydrazineyl)-5,6-diphenyl-1,2,4-triazine (7g)

Yellow solid: Yield %95; mp: 237–240 °C, IR (KBr, cm^{-1}) ν: 1080, 1168, 1243, 1500, 1608, 2950, 2961, 3482 .^{1}H NMR (500 MHz, DMSO-d_6) δ_H (ppm): 1.25 (s, 9H, −C (C<u>H</u>$_3$)$_3$), 5.19 (s, 2H, N−C<u>H</u>$_2$−Ph), 5.57 (s, 2H, C<u>H</u>$_2$−O−Ph), 7.11 (d, 2H, J = 8.5 Hz, Ar−<u>H</u>), 7.25 (d, J = 8.0 Hz, 2H, Ar−<u>H</u>), 7.37–7.46 (m, 10H, Ar−<u>H</u>), 7.48 (d, J = 8.0 Hz, 2H, Ar−<u>H</u>), 7.67 (d, 2H, J = 8.5 Hz, Ar−<u>H</u>), 8.24 (s, 1H, C=C<u>H</u>−N),

8.30 (s, 1H, N=C−H), 11.86 (s, 1H, N−H), ^{13}C NMR (125 MHz, DMSO-d_6) δ_c (ppm):31.5, 34.7, 53.0, 61.6, 115.6, 125.2, 126.0, 128.1, 128.2, 128.6, 128.7, 128.8, 129.5, 129.9, 130.7, 133.5, 136.6, 143.2, 143.7, 144.3, 147.6, 151.1, 156.8, 159.6. LC- MS (*m/z*): 594 [M^+].

4.1.14. Synthesis of (E)-3-(2-(4-((1-(3,4-dichlorobenzyl)-1H-1,2,3-triazol-4-yl) methoxy) benzylidene) hydrazineyl)-5,6-diphenyl-1,2,4-triazine (7h)

Yellow solid: Yield % 94; mp: 230–234 °C, IR (KBr, cm^{-1}) ν: 1049, 1082, 1185, 1360, 1504, 1735, 3045, 3148 . ^{1}H NMR (500 MHz, DMSO-d_6) δ_H (ppm): 5.21 (s, 2H, N−CH_2−Ph), 5.65 (s, 2H, CH_2−O−Ph), 7.11 (d, 2H, J = 8.3 Hz, Ar−H), 7.30–7.66 (m, 12H, Ar−H), 7.67 (d, 2H, J = 8.3 Hz, Ar−H), 7.95 (s, 1H, Ar−H), 8.24 (s, 1H, N=C−H), 8.36 (s, 1H, C=CH−N), 11.86 (s, 1H, N−H), ^{13}C NMR (125 MHz, DMSO-d_6) δ_c (ppm): 79.7, 81.9, 115.6, 117.3, 125.4, 128.2, 128.6, 128.7, 128.9, 129.5, 129.9, 130.6, 131.4, 131.5, 131.7, 136.5, 137.4, 137.9, 151.6, 152.4, 153.9, 159.5, 162.8. LC- MS (*m/z*): 606 [M^+].

4.1.15. Synthesis of (E)-3-(2-(4-((1-(3-chlorobenzyl)-1H-1,2,3-triazol-4-yl)methoxy) benzylidene) hydrazineyl)-5,6-diphenyl-1,2,4-triazine (7i)

Yellow solid, Yield; %87, mp: 241–245 °C , IR (KBr, cm^{-1}) ν: 1029, 1080, 1168, 1235, 1507, 1610, 2870, 3214. ^{1}H NMR (300 MHz, DMSO-d_6) δ_H (ppm): 5.21 (s, 2H, N−CH_2−Ph), 5.65 (s, 2H, CH_2−O−Ph), 7.10 (d, 2H, J = 7.2 Hz, Ar−H), 7.38–7.45 (m, 14H, Ar−H), 7.66 (d, 2H, J = 7.2 Hz, Ar−H), 8.24 (s, 1H, C=CH−N), 8.36 (s, 1H, N=C−H), 11.84 (s, 1H, N−H), ^{13}C NMR (125 MHz, DMSO-d_6) δ_c (ppm): 52.5, 61.7, 115.6, 125.4, 127.2, 128.2, 128.3, 128.9, 128.6, 128.7, 129.5, 129.9, 130.7, 131.2, 133.8, 136.5, 136.7, 138.9, 143.3, 144.3, 151.1, 156.8, 159.5. LC- MS (*m/z*): 572 [M^+].

4.1.16. Synthesis of (E)-2-(3-(4-((4-((2-(5,6-diphenyl-1,2,4-triazin-3-yl) hydrazono)methyl)phenoxy)methyl)-1H-1,2,3-triazol-1-yl)propyl) isoindoline-1,3-dione (7j)

Yellow solid, Yield; %85, mp: 240–243 °C, IR (KBr, cm^{-1}) ν : 1080, 1168, 1245, 1508, 1607, 1711, 1771, 2926, 3461. ^{1}H NMR (500 MHz, DMSO-d_6) δ_H (ppm): 2.19 (p, 2H, CH_2−CH_2−CH_2), 3.63 (t, 2H, CO−N−CH_2−CH_2), 4.45 (t, 2H, N=N−N−CH_2−CH_2), 5.18 (s, 2H, N−CH_2−Ph), 7.11 (d, 2H, J = 8.0 Hz, Ar−H), 7.37–7.49 (m, 10H, Ar−H), 7.67 (d, 2H, J = 8.0 Hz, Ar−H), 7.84–7.86 (m, 4H, Ar−H), 8.23 (s, 1H, C=CH−N), 8.26 (s, 1H, N=C−H), 11.85(s, 1H, N−H), ^{13}C NMR (125 MHz, DMSO-d_6) δ_c (ppm): 23.0, 63.1, 65.3, 76.2, 112.9, 115.5, 118.2, 123.5, 125.2, 128.6, 128.7, 129.5, 129.7, 129.9, 132.2, 134.8, 137.1, 144.7, 145.5, 147.0, 151.2, 156.5, 168.4. LC- MS (*m/z*): 635 [M^+].

4.2. BACE1 activity evaluations

The BACE1 FRET (fluorescence resonance energy transfer) assay kit was purchased from Invitrogen (former Pan Vera corporation, Madison, WI). Enzyme inhibition assay was carried out according to the manufacturer's instructions; the enzyme (purified baculovirus-expressed BACE1), substrate (Rh-EVNLDAEFK-Quencher) and test compounds (in DMSO) at different concentrations were diluted in the reaction buffer (50 mM sodium acetate, pH 4.5) to make 3X working solutions. The assay was carried out in a black 96-well microplate with a final volume of 30 μL consisting of equal amounts of 3X enzyme, substrate and test compound. The final concentration of DMSO was less than 6% (v/v). The reaction mixtures were incubated at 25 °C for 90 min in the dark and then 10 μL of the stop solution (2.5 M sodium acetate) was added to stop the reaction. Finally, the fluorescent intensity of the enzymatic product was measured using a multiwell spectrofluorometer instrument (BMG LABTECH, Polar star, Germany) capable of measuring at 544 nm excitation and 590 nm emission wavelengths [28]. Each experiment was repeated 4–5 times and the percentage of enzyme inhibition for each concentration of test compound was considered from the difference between the maximum enzyme activity wells (containing substrate plus enzyme) and baseline wells (containing substrate). CurveExpert software version 1.34 for Windows was used to calculate IC_{50} values from the concentration inhibition curves [20].

4.3. Assessment of antioxidant activity

The *in vitro* antioxidant activity of the synthesized compounds were tested by 1,1-diphenyl-2-picrylhydrazyl (DPPH) radical scavenging activity assay and using Quercetin as the reference compound. A screening was performed at the concentration of 10, 30 and 100 μM. The free radical scavenging activity of all synthesized compounds was determined by the DPPH assay. Several concentrations of the tested compounds dissolved in DMSO were added to DPPH solution in methanol (110 μM). The mixtures were left in the dark for 30 min and the absorbance of the solutions was measured at 517 nm by an UV/visible spectrophotometer. Measurements were carried out in triplicate for each experiment. The percentage of reduced DPPH was calculated by the following equation: (%) = 100 − [(Abs (control) − Abs (sample))/ Abs (control).

4.4. Assessment of neuroprotective activity against Aβ

Neuroprotective activity following exposure to Aβ and synthetic compounds was estimated using the MTT reduction assay. PC12 neuronal cells were plated in rat-tail collagen coated 96-well microplates at density of 5 * 10^5 cells/ml (100 ml in each well) and incubated for 48 h to adhere at 37 °C in humidified air containing 5% CO_2. Three to four different concentrations of test compounds were added to each well in triplicate and incubated for 3 h. Ten μl of human $A\beta_{25\text{-}35}$ was then added at a final concentration of 5 μM. At the end of the incubation time (24 h), 90 μL of the medium was replaced with 20 μL of 0.5 mg/ml MTT dissolved in RPMI containing phenol red and incubated for 2 h at 37 °C. Afterwards, formazan crystals were solubilized in 200 μL DMSO. The optical density was measured at 570 nm with background correction at 655 nm using a Bio-Rad microplate reader (Model 680, Bio-Rad). Stock solution of $A\beta_{25\text{-}35}$ was prepared by dissolution in distilled water to a 0.5 mM concentration [24]. Tested compounds were all first dissolved in DMSO and then diluted in the growth medium. For maintenance, two-thirds of the growth medium were changed every 4 days and the cells were sub-cultured once a week.

4.5. Assessment of metal-chelating effect

The metal chelation assay was carried out using a dual-beam UV–vis spectrophotometer Agilent 100 with 1 cm quartz cells. To investigate the metal binding ability of compound **7d** the UV absorption was recorded in the absence and presence of $ZnSO_4$, $FeSO_4$ with a wavelength ranging from 200 to 700 nm after incubating for 30 min at room temperature. The molar ratio method was performed to determine the stoichiometry of the complex. Final concentrations of the tested compound were 20 μM and the final concentrations of the metal ions ranging from 0 to 80 μM. Final volume of the reaction mixture was 1 ml. The UV spectra were normalized to the blank. The difference UV–Vis spectra were examined to investigate the ratio of 6d /metals in the complexes [22,24].

4.6. In silico studies

For molecular docking studies, 3D crystal structure of BACE1 (1w51) was retrieved from protein Data Bank. Water molecules and the cognate ligand were removed from the receptor and the hydrogen atoms were added and non-polar hydrogens were merged into related atoms of the receptor using ADT. The structures of the compounds were drawn using Chem3D Ultra 8.0 software. The energy minimizations were done by the semi-empirical MM^+ of HyperChem software [29].

The compounds were docked into the active site of proteins with default parameters. 100 runs for each ligand; 27,000 as maximum number of generations; 2,500,000 as maximum number of energy evaluations; 0.02 as rate of gene mutation and 0.8 as rate of crossover. The grid box was set with 50, 50, and 50 points in the x, y, and z directions, respectively, with the default grid spacing of 0.375 Å. All other options were set as default. Top-scored conformation was recorded for each compound and used for further analysis.

Acknowledgements

The authors wish to thank the financial support of the Ahvaz branch, Islamic Azad University, Ahvaz, Iran and National Institute for Medical Research Development, NIMAD (Grant No. 957334). We also thank Vice-Chancellor for Research, Shiraz University of Medical Sciences, Shiraz, Iran. We thank Alireza Edraki from Umass Medical School, MA, USA for thorough editing of this manuscript.

Appendix A. Supplementary material

Supplementary data to this article can be found online at https://doi.org/10.1016/j.bioorg.2018.11.038.

References

[1] 2018 Alzheimer's disease facts and figures, Alzheimer's & Dementia, 14(3) 2018, 367–429.
[2] R.J. Castellani, G. Perry, The complexities of the pathology–pathogenesis relationship in Alzheimer disease, Biochem. Pharmacol. 88 (4) (2014) 671–676.
[3] M.G. Savelieff, S. Lee, Y. Liu, M.H. Lim, Untangling amyloid-β, tau, and metals in Alzheimer's disease, ACS Chem. Biol. 8 (5) (2013) 856–865.
[4] L. Mucke, D.J. Selkoe, Neurotoxicity of amyloid β-protein: synaptic and network dysfunction, Cold Spring Harbor Perspect. Med. 2 (7) (2012) a006338.
[5] Y.-H. Liu, B. Giunta, H.-D. Zhou, J. Tan, Y.-J. Wang, Immunotherapy for Alzheimer disease—the challenge of adverse effects, Nat. Rev. Neurol. 8 (8) (2012) 465.
[6] H. Stower, Searching for Alzheimer's disease therapies, Nat. Med. 24 (7) (2018) 894–897.
[7] Y. Hamada, Y. Kiso, Discovery of BACE1 Inhibitors for the Treatment of Alzheimer's Disease, Quantitative Structure-Activity Relationship, InTech, 2017.
[8] W.J. Lukiw, Amyloid beta (Aβ) peptide modulators and other current treatment strategies for Alzheimer's disease (AD), Expert Opin. Emerg. Drugs 17 (1) (2012) 43–60.
[9] J.L. Cummings, R. Doody, C. Clark, Disease-modifying therapies for Alzheimer disease Challenges to early intervention, Neurology 69 (16) (2007) 1622–1634.
[10] G. Probst, Y.-Z. Xu, Small-molecule BACE1 inhibitors: a patent literature review (2006–2011), Expert Opin. Ther. Pat. 22 (5) (2012) 511–540.
[11] D. Amantea, Editorial overview: neurosciences: brain and immunity: new targets for neuroprotection, Curr. Opin. Pharmacol. 26 (2016) v.
[12] A. Robert, Y. Liu, M. Nguyen, B. Meunier, Regulation of copper and iron homeostasis by metal chelators: a possible chemotherapy for Alzheimer's disease, Acc. Chem. Res. 48 (5) (2015) 1332–1339.
[13] A. Kumar, C.M. Nisha, C. Silakari, I. Sharma, K. Anusha, N. Gupta, P. Nair, T. Tripathi, A. Kumar, Current and novel therapeutic molecules and targets in Alzheimer's disease, J. Formos. Med. Assoc. 115 (1) (2016) 3–10.
[14] M. Nguyen, A. Robert, A. Sournia-Saquet, L. Vendier, B. Meunier, Characterization of new specific copper chelators as potential drugs for the treatment of Alzheimer's disease, Chem.-A Eur. J. 20 (22) (2014) 6771–6785.
[15] D. Praticò, Oxidative stress hypothesis in Alzheimer's disease: a reappraisal, Trends Pharmacol. Sci. 29 (12) (2008) 609–615.
[16] W.R. Markesbery, Oxidative stress hypothesis in Alzheimer's disease, Free Radical Biol. Med. 23 (1) (1997) 134–147.
[17] E. Candelario-Jalil, Injury and repair mechanisms in ischemic stroke: considerations for the development of novel neurotherapeutics, Curr. Opin. Investig. Drugs 10 (7) (2009) 644–654.
[18] N. Edraki, O. Firuzi, A. Foroumadi, R. Miri, A. Madadkar-Sobhani, M. Khoshneviszadeh, A. Shafiee, Phenylimino-2H-chromen-3-carboxamide derivatives as novel small molecule inhibitors of β-secretase (BACE1), Bioorg. Med. Chem. 21 (8) (2013) 2396–2412.
[19] N. Edraki, O. Firuzi, Y. Fatahi, M. Mahdavi, M. Asadi, S. Emami, K. Divsalar, R. Miri, A. Iraji, M. Khoshneviszadeh, L. Firoozpour, A. Shafiee, A. Foroumadi, N-(2-(Piperazin-1-yl)phenyl)arylamide derivatives as β-secretase (BACE1) inhibitors: simple synthesis by Ugi four-component reaction and biological evaluation, Archiv der Pharmazie 348 (5) (2015) 330–337.
[20] S. Azimi, A. Zonouzi, O. Firuzi, A. Iraji, M. Saeedi, M. Mahdavi, N. Edraki, Discovery of imidazopyridines containing isoindoline-1,3-dione framework as a new class of BACE1 inhibitors: design, synthesis and SAR analysis, Eur. J. Med. Chem. 138 (2017) 729–737.
[21] J. Yuan, S. Venkatraman, Y. Zheng, B.M. McKeever, L.W. Dillard, S.B. Singh, Structure-based design of beta-site APP cleaving enzyme 1 (BACE1) inhibitors for the treatment of Alzheimer's disease, J. Med. Chem. 56 (11) (2013) 4156–4180.
[22] A. Iraji, O. Firuzi, M. Khoshneviszadeh, H. Nadri, N. Edraki, R. Miri, Synthesis and structure-activity relationship study of multi-target triazine derivatives as innovative candidates for treatment of Alzheimer's disease, Bioorg. Chem. 77 (2018) 223–235.
[23] M.R. Jones, J.R. Thompson, M.C. Wang, I.J. Kimsey, A.S. DeToma, A. Ramamoorthy, M.H. Lim, T. Storr, Dual-function triazole–pyridine derivatives as inhibitors of metal-induced amyloid-β aggregation, Metallomics 4 (9) (2012) 910–920.
[24] A. Iraji, O. Firuzi, M. Khoshneviszadeh, M. Tavakkoli, M. Mahdavi, H. Nadri, N. Edraki, R. Miri, Multifunctional iminochromene-2H-carboxamide derivatives containing different aminomethylene triazole with BACE1 inhibitory, neuroprotective and metal chelating properties targeting Alzheimer's disease, Eur. J. Med. Chem. 141 (2017) 690–702.
[25] M. Khoshneviszadeh, M.H. Ghahremani, A. Foroumadi, R. Miri, O. Firuzi, A. Madadkar-Sobhani, N. Edraki, M. Parsa, A. Shafiee, Design, synthesis and biological evaluation of novel anti-cytokine 1,2,4-triazine derivatives, Bioorg. Med. Chem. 21 (21) (2013) 6708–6717.
[26] R.J. O'Brien, P.C. Wong, Amyloid precursor protein processing and Alzheimer's disease, Annu. Rev. Neurosci. 34 (2011) 185–204.
[27] Z. Haghighijoo, O. Firuzi, B. Hemmateenejad, S. Emami, N. Edraki, R. Miri, Synthesis and biological evaluation of quinazolinone-based hydrazones with potential use in Alzheimer's disease, Bioorg. Chem. 74 (2017) 126–133.
[28] A. Sara, F. Omidreza, I. Aida, Z. Afsaneh, K. Mahsima, M. Mohammad, E. Najmeh, Synthesis and in vitro biological activity evaluation of novel imidazo[2,1-b][1,3,4] thiadiazole as anti-Alzheimer agents, Lett. Drug Des. Discovery 16 (2019) 1-1.
[29] N. Edraki, A. Iraji, O. Firuzi, Y. Fattahi, M. Mahdavi, A. Foroumadi, M. Khoshneviszadeh, A. Shafiee, R. Miri, 2-Imino 2H-chromene and 2-(phenylimino) 2H-chromene 3-aryl carboxamide derivatives as novel cytotoxic agents: synthesis, biological assay, and molecular docking study, J. Iran. Chem. Soc. 13 (12) (2016) 2163–2171.